

# Gilteritinib reverses ABCB1-mediated multidrug resistance: Preclinical in vitro and animal investigations

Meng Zhang<sup>a,1</sup>, Mei-Ling She<sup>b,1</sup>, Jun Chen<sup>a,1</sup>, Xiao-Qi Zeng<sup>a</sup>, Qing-Quan Xiong<sup>a</sup>, Ying-Huan Cen<sup>a</sup>, Jia-An Ye<sup>a</sup>, Guo-Bin Qiu<sup>a,\*</sup>, Shu-Yi Yang<sup>a,\*</sup>, Guang-Hui Ren<sup>a,\*</sup>

<sup>a</sup> Department of Thyroid And Breast Surgery, Shenzhen Hospital of Southern Medical University, Shenzhen, Guangdong 510000, China

<sup>b</sup> Department of Gastroenterology, Xiyuan Hospital, China Academy of Chinese Medical Sciences, Beijing 100020, China

## ARTICLE INFO

### Keywords:

ABCB1 transporter  
Cancer chemotherapy  
FLT3 inhibitor  
Gilteritinib  
Multidrug resistance  
Preclinical studies

## ABSTRACT

Multi-drug resistance (MDR) poses a significant challenge to cancer treatment. Targeting ATP-binding cassette subfamily B member 1 (ABCB1) is a viable strategy for overcoming MDR. This study examined the preclinical in vitro and animal studies that used gilteritinib, a FLT3 inhibitor that reverses ABCB1-mediated MDR. At nontoxic levels, gilteritinib significantly increased the susceptibility of cancer cells overexpressing ABCB1 to chemotherapeutic drugs. Furthermore, it impaired the development of drug-resistant cell colonies and 3D spheroids. Studies on the reversal mechanism have shown that gilteritinib can directly bind to the drug-binding site of ABCB1, inhibiting drug efflux activity. Consequently, the substrate's drug cytotoxicity increases in MDR cells. Furthermore, gilteritinib increased ATPase activity while leaving ABCB1 expression and subcellular distribution unchanged and inhibited AKT or ERK activation. Docking analysis indicated that Gilteritinib could interact with the drug-binding site of the ABCB1 transporter. In vivo studies have shown that gilteritinib improves the anti-tumor efficacy of paclitaxel in nude mice without obvious toxic effects. In conclusion, our preclinical investigations show that gilteritinib has the potential to successfully overcome ABCB1-mediated MDR in a clinical environment when combined with substrate medicines.

## 1. Introduction

The high incidence of malignant tumors significantly affects human well-being and physical condition [1]. Chemotherapy has contributed substantially to tumor treatment. However, the development of multidrug resistance (MDR) during treatment has become a significant obstacle, reducing tumor treatment efficacy and potentially causing chemotherapy to fail [2,3]. Tumor MDR not only exacerbates the suffering of patients with cancer but also complicates cancer treatment [4–6]. The multidrug process of MDR is complex, involving several components and intracellular pathways. These include decreased medication absorption into cells [7], enhanced expulsion of energy-dependent pharmaceuticals [8], changes in drug action sites [9], increased detoxification system activity, and overactivation of anti-apoptotic pathways [10]. The increased expression of drug

transporters on tumor cell membranes, including efflux "pumps" such as ABCB1 (ATP-binding cassette subfamily B member 1) and ABCG2 (ATP-binding cassette subfamily G member 2) and ABCC1 (ATP Binding Cassette Subfamily C Member 1), is an important mechanism contributing to treatment resistance [4,11]. The ATP-binding cassette (ABC) transporter superfamily is a vast collection of transmembrane proteins that can be categorized into seven subtypes (ABCA-ABCG) according to the homology of conserved region sequences. ABCB1, ABCG2, and ABCC1 are the primary subfamily proteins that influence the MDR on the cell membrane of tumor cells [12–14]. To achieve transport against a concentration gradient, these transporters use adenosine triphosphate (ATP) to pump structurally dissimilar substrate drugs out of the cell, lowering drug concentrations below the action threshold and resulting in cell resistance [15,16].

The overexpression of ABCB1 may result in a reduction of

**Abbreviations:** MDR, multidrug resistance; ABCB1, ATP-binding cassette subfamily B member 1; ABCG2, ATP-binding cassette subfamily G member 2; ATP, adenosine triphosphate; FLT3, fms-like tyrosine kinase 3; AML, acute myeloid leukemia; HE, Hematoxylin and Eosin; PTX, Paclitaxel, DOX, Doxorubicin; CETSA, Cellular Thermal Shift Assay; AKT, protein kinase B; ERK, extracellular signal-regulated kinase.

\* Corresponding authors.

E-mail addresses: [gbqiu1@qq.com](mailto:gbqiu1@qq.com) (G.-B. Qiu), [yangshuyi7788@163.com](mailto:yangshuyi7788@163.com) (S.-Y. Yang), [doctorren1218@hotmail.com](mailto:doctorren1218@hotmail.com) (G.-H. Ren).

<sup>1</sup> These authors contributed equally.

<https://doi.org/10.1016/j.bioph.2024.117603>

Received 27 August 2024; Received in revised form 15 October 2024; Accepted 21 October 2024

Available online 30 October 2024

0753-3322/© 2024 The Author(s). Published by Elsevier Masson SAS. This is an open access article under the CC BY-NC license (<http://creativecommons.org/licenses/by-nc/4.0/>).

intracellular substrate medicines, the recognized substrates of the ABCB1 transporter protein include doxorubicin, paclitaxel, colchicine, and vincristine. Consequently, targeting ABCB1 is considered one of an effective method for eliminating MDR, as it is the most extensively studied MDR transporter [17]. Various ABCB1 inhibitors have been identified and developed in response to this factor [18]. Verapamil [19] and cyclosporine A [20] are known as chemosensitizers that inhibit ABCB1. These chemosensitizers compete with or selectively bind to ABCB1, limiting anti-tumor drug efflux [21]. However, toxicity and other constraints preclude their approval for clinical use [22–24]. Consequently, it is critical to develop ABCB1 reversal agents that are both highly effective and specific.

Fms-like tyrosine kinase 3 (FLT3) is a member of the class III receptor tyrosine kinase family, and its ligand regulates pluripotent stem cell growth, survival, and specialization. FLT3 mutations are a common genetic modification in acute myeloid leukemia (AML) [25,26]. Gilteritinib is an oral small-molecule FLT3 inhibitor that functions as an antitumor agent. It is licensed for the treatment of FLT3 mutation-positive acute myeloid leukemia in the United States, Canada, Europe, Brazil, South Korea, and Japan [27–29]. Our group has conducted extensive research on ABCB1 inhibitors [19,30,31]. This study reports preclinical findings on the efficacy of gilteritinib in reversing ABCB1-mediated MDR.

## 2. Material and methods

### 2.1. Chemical compounds

We acquired Gilteritinib (HPLC purity: 99.34 %), Paclitaxel (PTX), Doxorubicin (DOX), cisplatin, and verapamil from MedChemExpress (Monmouth Junction, NJ, USA). Gibco (Carlsbad, California, USA) supplied DMEM and fetal bovine serum (FBS). Sigma-Aldrich (St. Louis, MO, USA) provided monoclonal antibodies against ABCB1, AKT, p-AKT, ERK, p-ERK, GAPDH, and Alexa Fluor 488 conjugated antibodies, which are widely used and well-established antibodies for detecting and assessing ABCB1 protein expression. Unless otherwise specified, all the reagents were acquired from Meilun Biotechnology (Dalian, China).

### 2.2. Cell lines and cell culture

The multidrug-resistant ABCB1-overexpressing cell lines MCF7/ADR and SW620/Ad300 were created by treating human breast carcinoma cell line MCF7 and human colon carcinoma cell line SW620 cells with DOX. HEK293/pcDNA3.1 and HEK293/ABCB1 cells from human embryonic kidney HEK293 cells were transfected with an empty vector and one containing the full-length ABCB1 gene. These cells were cultured at 37 °C in a humid incubator containing 5 % CO<sub>2</sub>.

### 2.3. CCK-8 assay

The CCK8 assay was used to determine drug cytotoxicity *in vitro* [19]. Cells in the logarithmic growth phase were seeded into 96-well plates at  $5 \times 10^3$ /well. Once the cell attachment, the appropriate treatment was administered. Gilteritinib was serially diluted (0–100  $\mu$ M) and injected into the specified wells for cytotoxicity testing. In reversal studies, Gilteritinib (0.1 or 0.3  $\mu$ M) or Verapamil (0.3 or 3  $\mu$ M), a positive control that blocks ABCB1, were added two hours before stronger conventional anticancer drugs. After treatment, we added 20  $\mu$ l of CCK-8 solution to each culture well and incubated the plate for 2 h. An enzyme-labeled instrument was used to measure the absorbance (A) of each well at 570 nm.

### 2.4. Colony formation assay

During the logarithmic growth phase, MCF-7/ADR cells received Gilteritinib (0.3  $\mu$ mol/L, 4 h), PTX (1  $\mu$ mol/L, 2 h), or both (Gilteritinib

was added for 2 h, and then PTX and Gilteritinib were added for 2 h). Following treatment, the cells were seeded in 6-well plates at a density of 1000 cells per well. The growth medium was replaced every three days, and the cells were incubated for seven days. The cells were washed with PBS and then fixed with methanol for 30 min before staining them with a 0.1 % crystal violet solution for another 30 min. After washing and drying, the cells were examined under a microscope to determine the pace of colony development and to capture images. Quantitative analysis was then conducted using ImageJ software (NIH, MD).

### 2.5. 3D spheroid assay

MCF-7/ADR cells were treated with Gilteritinib alone (0.3  $\mu$ mol/L, 4 h), PTX alone (1  $\mu$ mol/L, 2 h), or a combination of Gilteritinib and PTX (pre-incubation with Gilteritinib for 2 h, followed by treatment with PTX plus Gilteritinib for 2 h). The cells were then placed in DMEM/F12 medium supplemented with B27, EGF, bFGF, and heparin before being transferred to 96-well plates with a low attachment surface. The size of the 3D spheroids was measured on day 7.

### 2.6. Doxorubicin accumulation and efflux assay

Accumulation and efflux tests were performed using FACSort flow cytometry, and the results were analyzed using FlowJo V10. Samples were prepared by dividing MCF7 and MCF7/ADR cells into treatment groups of  $2 \times 10^5$  cells. The cells were incubated with verapamil or gilteritinib for 2 h. Each treatment group received 5  $\mu$ mol/L of doxorubicin, with or without verapamil or gilteritinib. Before analysis, the cells were centrifuged at 500 g and reconstituted in 300  $\mu$ L of PBS solution containing 0.5 % BSA.

### 2.7. ATPase assay

An SB-MDR1-Hi5-PREDEASY-ATPase kit (Sigma Chemical Co., St. Louis, MO, USA) was used to measure the ATPase activity associated with ABCB1 using previously established methods [32].

### 2.8. Western Blot Assay

Proteins from each group were extracted using a lysis buffer, and the protein concentrations were determined using the BCA method. Equal quantities of protein samples were electrophoretically separated using sodium dodecyl sulfate-polyacrylamide gels. Subsequently, the proteins were transferred to PVDF membranes. After adding 5 % skim milk, the membrane was washed three times with TBST. Then the membrane was incubated in monoclonal primary mouse antibodies against GAPDH (1:1000) or ABCB1 (1:1000) overnight, and then followed by incubation with HRP conjugated rabbit anti-mouse IgG secondary antibody (1:1000)

for 1 h. The membrane was processed using the ECL luminescence method after washing, and the resulting images were examined using the ImageJ software.

### 2.9. Immunofluorescence assay

The cells were cultivated in conical dishes composed of a glass matrix. They were exposed to 0.3  $\mu$ M Gilteritinib for 48 h. The cells were then washed three times with PBS and immobilized using paraformaldehyde for 15 min. Membranes were rendered permeable by applying a 0.1 % Triton X-100 solution and then closed off with a 1 % BSA solution. The primary antibodies were incubated overnight, whereas the secondary antibodies were incubated for 1 h. DAPI staining was performed, and images were captured using a Zeiss LSM 880 confocal microscope (Carl Zeiss IQS, Oberkochen, Germany).

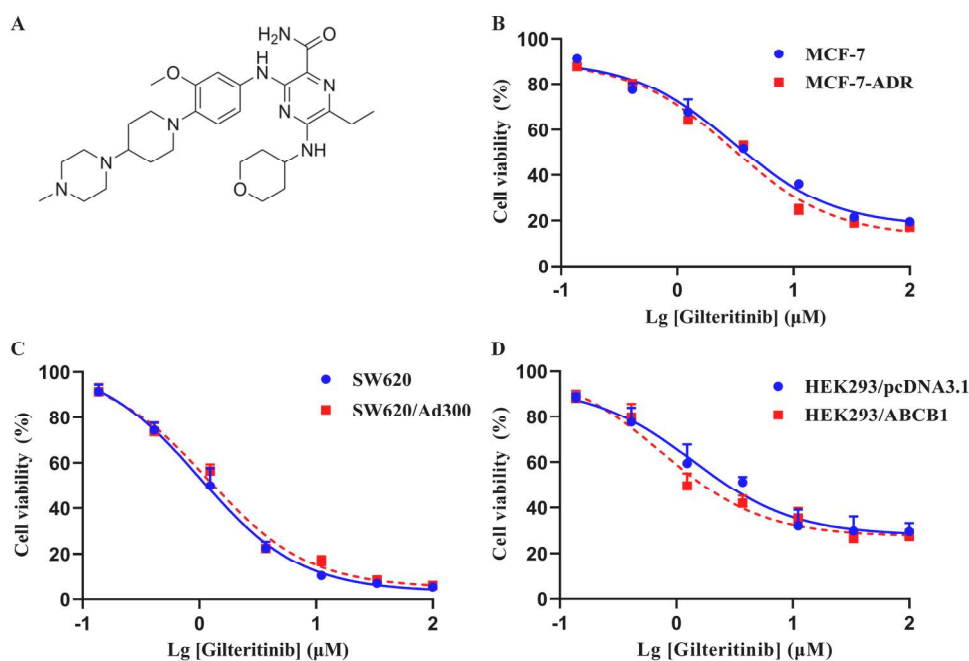


**Fig. 1.** The cytotoxicity of Giliteritinib in parental and drug-resistant cells. (A) Chemical structure of Giliteritinib. Cell viability curves for (B-C) MCF7, MCF7/ADR, SW620, and SW620/AD300 cells. (D) HEK293/pcDNA3.1, HEK293/ABCB1. For three independent assays, data are presented as mean  $\pm$  SD.

## 2.10. Cellular thermal shift assay (CETSA)

MCF7/ADR cells were collected, and the cell solution underwent five cycles of freezing and thawing using liquid nitrogen. After centrifugation, the liquid remaining on top was divided into two equal aliquots. One aliquot was exposed to a 0.3  $\mu\text{mol/L}$  giliteritinib solution, while the other aliquot was exposed to a solvent control containing an equivalent amount of DMSO (1 %, v/v). After a 30-minute incubation at room temperature, the supernatant was divided into smaller portions and subjected to varying temperatures for 3 min. After centrifugation, the liquid component containing the desired substances was collected and analyzed using a western blot.

## 2.11. Molecular docking

Molecular docking was performed on giliteritinib using a model of human ABCB1, following an established method. Briefly, the human ABCB1 protein model (7A69) was acquired from the RCSB Protein Data Bank, and the molecular structure of giliteritinib was retrieved through PubChem. The docking calculation was performed using Maestro v. 11.1 software (Schrodinger Inc., New York, NY, USA). Once the receptor and ligand were created, Glide XP docking was executed, followed by induced-fit docking using the default technique.

## 2.12. MDR xenograft tumor models

To confirm the *in vivo* reversal effect of giliteritinib, a xenograft tumor model with MDR was developed in female nude BALB/c mice aged 4–6 weeks obtained from the Guangdong Medical Experimental Animal Center. This procedure was performed in accordance with the methods outlined in earlier studies [32,33]. The giliteritinib concentration was chosen based on past animal and clinical research to ensure safety and feasibility [34]. The study was conducted according to the criteria of the Declaration of Helsinki and was approved by the Ethics Committee of Shenzhen Hospital of Southern Medical University (NO. 2024-0037).

Nude mice received subcutaneous injections of  $1 \times 10^7$  MCF7 cells or  $1 \times 10^7$  MCF7/ADR cells. The mice were divided into four treatment groups, with 6 mice in each group, using a random assignment method:

(1) a control group that received 10 mg/kg of saline orally; (2) a group that received 10 mg/kg of giliteritinib orally; (3) a group that received 18 mg/kg of PTX intraperitoneally; and (4) a group that received 18 mg/kg of PTX intraperitoneally and 10 mg/kg of giliteritinib orally. All the mice were dosed every three days for a total of four doses. Giliteritinib was administered orally one hour before injecting PTX. The treatments were administered at intervals of three days for a total of 15 days.

Every three days, the body weight and tumor volume of the mice were measured. Tumor volume (V) was calculated using the following formula:  $V = (\text{length} \times \text{width}^2) \times 0.5$ . Tumor inhibition rate (IR %) =  $(1 - \text{average tumor weight of the experimental group} / \text{average tumor weight of the control group}) \times 100$  %. Once the tumor had attained an average diameter of 50 mm<sup>3</sup>, the experiment was concluded and blood was drawn from the eyeballs of the mice. Finally, all mice were rendered unconscious using carbon dioxide and euthanized, after which tumor xenografts were excised and weighed.

## 2.13. Hematoxylin and eosin (HE) staining

The dewaxed slices made from tumor xenografts were stained with hematoxylin for 10 min, then rinsed and stained with eosin for 3 min. After removing the water with varying concentrations of ethanol, tissues without wax were immersed in xylene and sealed with neutral balsam [32].

## 2.14. Serum biochemical assay

After concluding the treatments, blood samples were drawn from the ocular regions of the mice. Blood samples were analyzed using a completely automated biochemical analyzer (Chemray 800, Raydo, Shenzhen, China).

## 2.15. Statistical analysis

Statistical analyses were conducted utilizing SPSS statistical software (version 27.0, Chicago, IL, USA). Data were presented as the mean  $\pm$  standard deviation (SD) of three independent experiments. Statistical tests for data analysis included one-way ANOVA and Wilcoxon rank sum

**Table 1**  
The cytotoxicity of Gilteritinib in parental and ABCB1-overexpressing cells.

Cell lines	IC50 ± SD <sup>a</sup> (RF <sup>b</sup> ) (μM)		HEK293/ABCB1	SW620	SW620/Ad300	MCF7	MCF7/ADR
	HEK293/pcDNA3.1	HEK293/ABCB1					
<b>Doxorubicin</b>							
+Verapamil (3 μM)	0.351 ± 0.007 (1.000)	1.3457 ± 0.273 (38.378)	0.256 ± 0.003 (1.000)	13.968 ± 0.139 (54.486)	1.364 ± 0.019 (1.000)	43.407 ± 0.241 (31.817)	
+Verapamil (0.3 μM)	0.304 ± 0.011 (0.866)	0.414 ± 0.003 (1.180)*	0.280 ± 0.006 (1.092)	0.315 ± 0.013 (1.227)*	1.335 ± 0.018 (0.978)	1.645 ± 0.019 (1.206)*	
+Gilteritinib (0.3 μM)	0.385 ± 0.004 (1.097)	1.649 ± 0.008 (4.702)*	0.305 ± 0.004 (1.190)	1.139 ± 0.029 (4.445)*	1.279 ± 0.008 (0.937)	6.236 ± 0.021 (4.457)*	
+Gilteritinib (0.3 μM)	0.303 ± 0.001 (0.865)	0.733 ± 0.001 (2.091)*	0.267 ± 0.007 (1.043)	0.552 ± 0.005 (2.154)*	1.235 ± 0.006 (0.905)	4.488 ± 0.034 (3.290)*	
+Gilteritinib (0.1 μM)	0.299 ± 0.008 (0.852)	2.737 ± 0.053 (7.805)*	0.247 ± 0.001 (0.962)	2.353 ± 0.026 (9.179)*	1.336 ± 0.010 (0.979)	10.054 ± 0.220 (7.369)*	
<b>Paclitaxel</b>							
+Verapamil (3 μM)	0.459 ± 0.238 (1.000)	30.086 ± 0.982 (49.017)	0.235 ± 0.003 (1.000)	13.352 ± 0.100 (56.895)	0.702 ± 0.002 (1.000)	18.980 ± 0.372 (27.054)	
+Verapamil (0.3 μM)	0.479 ± 0.008 (1.101)	0.741 ± 0.005 (1.206)*	0.248 ± 0.002 (1.057)	0.309 ± 0.009 (1.315)*	0.754 ± 0.003 (1.075)	0.750 ± 0.017 (1.070)*	
+Gilteritinib (0.3 μM)	0.446 ± 0.007 (1.075)	3.454 ± 0.021 (5.628)*	0.310 ± 0.007 (1.320)	1.059 ± 0.035 (4.514)*	0.668 ± 0.002 (0.953)	3.400 ± 0.043 (4.847)*	
+Gilteritinib (0.3 μM)	0.604 ± 0.005 (1.14)	1.568 ± 0.002 (2.555)*	0.358 ± 0.006 (1.525)	0.573 ± 0.008 (2.443)*	0.743 ± 0.004 (1.060)	1.467 ± 0.032 (2.091)*	
+Gilteritinib (0.1 μM)	1.604 ± 0.011 (1.072)	4.845 ± 0.022 (7.894)*	0.357 ± 0.002 (1.520)	2.006 ± 0.029 (8.547)*	0.705 ± 0.007 (1.005)	5.842 ± 0.144 (8.326)*	
<b>Cisplatin</b>							
+Verapamil (3 μM)	1.609 ± 0.025 (1.000)	1.730 ± 0.021 (1.075)	2.220 ± 0.013 (1.000)	2.842 ± 0.027 (1.280)	7.459 ± 0.028 (1.000)	8.333 ± 0.015 (1.117)	
+Verapamil (0.3 μM)	1.471 ± 0.021 (0.931)	1.865 ± 0.010 (1.159)	2.255 ± 0.030 (1.016)	2.130 ± 0.039 (0.959)	7.888 ± 0.065 (1.058)	7.674 ± 0.278 (1.029)	
+Gilteritinib (0.3 μM)	1.520 ± 0.017 (0.967)	1.643 ± 0.013 (1.022)	2.948 ± 0.032 (1.328)	2.340 ± 0.014 (1.054)	8.408 ± 0.025 (1.127)	7.169 ± 0.054 (0.961)	
+Gilteritinib (0.1 μM)	1.476 ± 0.031 (0.921)	1.632 ± 0.021 (1.014)	2.151 ± 0.017 (0.969)	2.242 ± 0.010 (1.010)	8.139 ± 0.033 (1.091)	9.117 ± 0.066 (1.222)	
+Gilteritinib (0.1 μM)	1.453 ± 0.021 (0.812)	1.835 ± 0.030 (1.141)	2.370 ± 0.017 (1.068)	2.427 ± 0.012 (1.093)	9.415 ± 0.009 (1.262)	9.433 ± 0.044 (1.265)	

<sup>a</sup> Values for the IC50 are shown as mean ± SD of at least three independent tests.

<sup>b</sup> By dividing the IC50 values of substrates with or without of inhibitor by the IC50 of parental cells without inhibitor, the resistance fold was computed.

\*  $P < 0.05$  vs. control treatment.

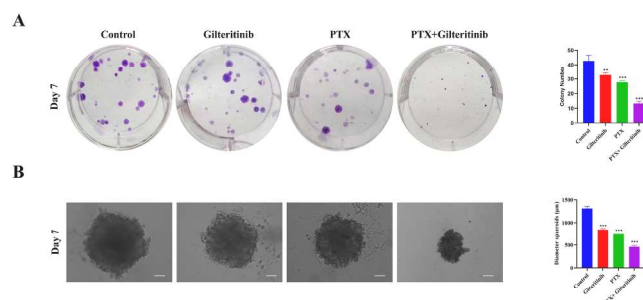


**Fig. 2.** Gilteritinib potentiated the inhibitory impact of PTX on colony and 3D spheroid formation. (A) Colony formation of MCF7/ADR cells was assessed following treatment with Gilteritinib (0.3 μmol/L), PTX (1 μmol/L), or a combination of both. (B) On day 7, the development of 3D spheroids by MCF7/ADR cells was observed after treatment with Gilteritinib (0.3 μmol/L), PTX (1 μmol/L), or a combination of both. The scale bar is 100 μm. All these experiments were repeated at least three times. Data are presented as the mean ± SD. (n = 3). \*\*  $p < 0.01$ , \*\*\*  $p < 0.001$  versus the corresponding control group.

test. Dunnett's post hoc test was used after ANOVA when multiple groups were compared with one control group. All tests were two-sided, and statistical significance was defined as a  $p$ -value below 0.05. Figures were produced utilizing GraphPad Prism 9 software (GraphPad Software, La Jolla, CA).

### 3. Results

#### 3.1. Gilteritinib reverses ABCB1-mediated MDR In Vitro

We used the CCK8 assay to determine the effect of gilteritinib on the proliferative activity of the cell lines used in this investigation. A curve was generated after 72 h of gilteritinib treatment (Fig. 1), indicating inhibition of cell proliferation. To prevent tumor MDR caused by toxic effects, we chose the concentration of Gilteritinib to be 0.3 μmol/L, resulting in a cell survival rate above 80 %. The trial doses of gilteritinib were therefore 0.3 μmol/L and 0.1 μmol/L. The results of the reversal resistance experiment demonstrated that in ABCB1-overexpressing cells (MCF-7/ADR and SW620/Ad300 cells) demonstrate resistance to chemotherapy drugs, with resistance fold values ranging from 54 to 57 (SW620/Ad300 cells) and 27–32 (MCF-7/ADR). Pre-treatment with gilteritinib significantly lowers the IC50 of all three chemotherapy agents in cancer cells. Gilteritinib increased the efficiency of anticancer drugs (DOX and PTX), which are ABCB1 substrates, in ABCB1-overexpressing cells (MCF-7/ADR and SW620/Ad300 cells). Furthermore, gilteritinib did not affect the sensitivity of normal cells to chemotherapeutic drugs. These findings were subsequently validated in HEK293/ABCB1 cells that had been genetically engineered to express ABCB1 (\*  $p < 0.05$ , Table 1). Cisplatin does not interact with ABCB1, hence it was used as a negative control. This finding suggests that gilteritinib can specifically enhance ABCB1-mediated MDR in laboratory settings.

#### 3.2. Gilteritinib coupled with PTX suppresses the growth of ABCB1-overexpressing cells

We used colony assays and 3D microsphere culture to investigate the effects of gilteritinib, either alone or in combination with PTX, on the proliferative potential of drug-resistant cells. Fig. 2A shows that gilteritinib significantly enhanced the inhibitory effect of PTX on SW620/Ad300 cell colony formation, outperforming the effects of gilteritinib and PTX alone (\*  $p < 0.05$ , \*\*  $p < 0.01$ , vs. control group). The 3D microsphere culture data showed that the combination of gilteritinib and PTX significantly reduced the average diameter of SW620/Ad300 spheroids compared to PTX alone (\*  $p < 0.05$  versus control group, Fig. 2B). These findings indicated that the combination of gilteritinib



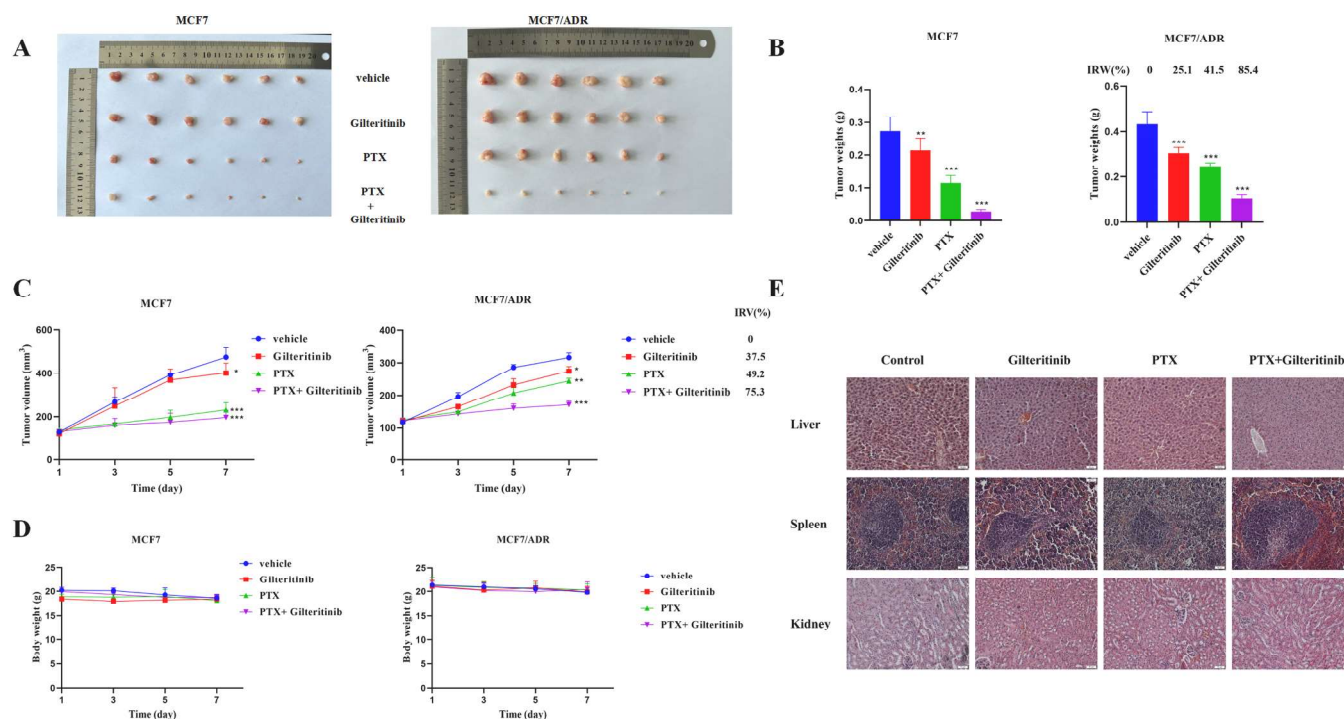


**Fig. 3.** Giliteritinib's antitumor efficacy in tumor xenograft models. (A) Picture of the removed tumors at the conclusion of the trial. (B) The weight of the tumor tissues at the conclusion of treatment. (C) Tumor volume at the conclusion of treatment. (D) Changes in mouse body weight throughout therapy. (E) HE analysis of Liver, Spleen and Kidney. All the data are presented as the mean ± SD. (n = 6). \*  $p < 0.05$ , \*\*  $p < 0.01$ , \*\*\*  $p < 0.001$  versus the corresponding control group. HE staining scale bar was 50  $\mu\text{m}$ .

**Table 2**  
Blood biochemical analysis.

Item	Value <sup>a</sup>			
	Vehicle	Giliteritinib	PTX	PTX+ Giliteritinib
Albumin, g/L	22.60 ± 1.23	21.80 ± 1.01	23.20 ± 3.41	24.30 ± 2.19
Total protein, g/L	53.60 ± 3.45	47.50 ± 2.42	57.90 ± 4.11	49.20 ± 3.22
Globulin, g/L	31.00 ± 1.13	25.70 ± 1.35	34.70 ± 2.91	24.90 ± 1.97
Alanine aminotransferase, U/L	48.00 ± 3.32	41.00 ± 2.76	47.00 ± 4.69	49.00 ± 11.43
Alkaline phosphatase, U/L	98.00 ± 7.55	111.00 ± 5.23	113.00 ± 11.24	129.00 ± 12.54
Urea nitrogen, mmol/L	8.79 ± 1.01	6.87 ± 1.09	8.04 ± 1.11	5.79 ± 0.98
Creatinine, umol/L	32.56 ± 1.55	26.28 ± 1.15	19.98 ± 1.23	20.45 ± 1.25
Blood glucose, mmol/L	5.27 ± 0.55	6.70 ± 0.37	5.20 ± 0.33	7.01 ± 0.24

<sup>a</sup> Date are presented as mean ± SD of at least three independent tests.

and PTX successfully inhibited SW620/Ad300 cell growth.

### 3.3. Giliteritinib synergistically enhances the antitumor effect of PTX in PDX models

We used a nude mouse xenograft tumor model to study giliteritinib's potential for reversing drug resistance *in vivo*. The model involved MCF7/ADR cells that had been genetically modified to overexpress ABCB1. The combination of PTX and giliteritinib effectively suppressed the growth of multidrug-resistant (MDR) tumors and provided more antitumor benefits than either PTX or giliteritinib alone (Fig. 3A). Following treatment, the tumors' weight and volume decreased

significantly, combination therapy has a more significant anti-tumor effect than monotherapy, with 75.29 % IRW and 85.4 % IRV (\*  $p < 0.05$ , \*\*  $p < 0.01$ , \*\*\*  $p < 0.001$  versus vehicle group, Fig. 3B, C). These decreases differed significantly from the groups that received only one form of treatment. Throughout the dosage period, the body weights of the nude mice in all four groups did not substantially decrease, and no notable differences were observed between the groups (Fig. 3D). To further assess the safety of giliteritinib, we stained the liver, spleen, and kidney tissues with HE. None of these organs showed visible abnormalities (Fig. 3E), indicating that combination treatment had no apparent adverse effects. Albumin, total protein, alanine aminotransferase, urea nitrogen, and creatinine levels were within the normal ranges. This implies that administering giliteritinib, PTX, or their combination did not affect liver and kidney function (Table 2). Routine blood tests indicated no significant differences in the various parameters (Table 3), suggesting that giliteritinib is both effective and safe as a medication-resistant reversal therapy in animal models of transplanted malignancies.

### 3.4. Giliteritinib increases DOX accumulation in ABCB1-overexpressing cells by reducing DOX Efflux

We conducted additional tests using flow cytometry to examine the effects of giliteritinib on ABCB1 transporter activity. Pretreatment of MCF7/ADR cells with 0.3  $\mu\text{M}$  giliteritinib resulted in a dose-dependent increase in DOX accumulation (Fig. 4B). However, giliteritinib did not affect ABCB1 transporter's function in the parental cell line MCF7 (Fig. 4A). The degree of DOX accumulation had no substantial impact, and its trend was similar to that of the positive control, verapamil. As a result, the aforementioned experimental data show that giliteritinib promotes the accumulation of chemotherapeutic drugs in cells over-expressing ABCB1.

Drug efflux tests were performed to determine whether the suppression of substrate drug efflux was the cause and to evaluate the

**Table 3**  
Blood routine analysis.

Item	Value <sup>a</sup>			
	Vehicle	Gilteritinib	PTX	PTX+ Gilteritinib
White blood cell, 10 <sup>9</sup> /L	3.30 ± 1.02	3.30 ± 1.03	2.20 ± 1.01	2.40 ± 1.01
Lymphocyte count, 10 <sup>9</sup> /L	3.40 ± 1.02	3.90 ± 1.02	3.20 ± 1.01	3.20 ± 1.01
Monocyte count, 10 <sup>9</sup> /L	0.10 ± 0.03	0.10 ± 0.01	0.10 ± 0.01	0.10 ± 0.02
Neutrophil count, 10 <sup>9</sup> /L	0.70 ± 0.34	0.80 ± 0.12	0.80 ± 0.23	0.90 ± 0.11
Percentage of Lymphocyte, %	65.20 ± 13.12	67.90 ± 10.76	61.20 ± 14.02	67.90 ± 13.43
Percentage of Monocyte, %	4.20 ± 0.65	4.50 ± 0.41	4.50 ± 0.36	4.30 ± 0.54
Percentage of Neutrophil, %	23.10 ± 1.55	31.30 ± 1.67	33.45 ± 1.02	34.10 ± 1.23
Red blood cell, 10 <sup>12</sup> /L	9.38 ± 2.10	9.36 ± 1.92	8.43 ± 1.44	7.23 ± 1.22
Hemoglobin concentration, g/L	121.00 ± 10.52	123.00 ± 12.02	131.00 ± 19.02	131.00 ± 25.76
Red blood specific volume, %	40.10 ± 3.31	41.10 ± 7.03	41.20 ± 6.54	44.30 ± 3.54
Mean corpuscular volume, fL	49.80 ± 4.76	46.20 ± 2.54	48.50 ± 4.12	47.00 ± 4.45
Mean corpuscular hemoglobin, pg	16.00 ± 2.64	16.30 ± 1.78	15.90 ± 1.79	16.20 ± 2.01
Mean corpuscular hemoglobin concentration, g/L	314.00 ± 20.21	321.00 ± 49.21	344.00 ± 31.55	313.00 ± 25.87
Red blood cell volume distribution, %	14.80 ± 1.71	14.90 ± 1.11	14.80 ± 1.02	14.90 ± 1.76
Platelet count, 10 <sup>12</sup> /L	1111.00 ± 50.89	1294.00 ± 92.02	1055.00 ± 69.02	1344.00 ± 120.65
Mean platelet volume, fL	4.60 ± 0.26	4.60 ± 0.13	4.30 ± 0.23	4.60 ± 0.33
Urea, mmol/L	8.79 ± 1.01	6.87 ± 1.09	8.04 ± 1.11	5.79 ± 0.98
CREA, umol/L	32.56 ± 1.55	26.28 ± 1.15	19.98 ± 1.23	20.45 ± 1.25

<sup>a</sup> Data are presented as mean ± SD of at least three independent tests.

impact of gilteritinib on the ability of drug-resistant cells to expel chemotherapeutic drugs. Following gilteritinib treatment for 0, 30, 60, and 90 min, DOX levels in drug-resistant MCF7/ADR cells were considerably higher than those in the control group (\*  $p < 0.05$ , Fig. 4D). This suggests that the amount of pumped DOX was significantly lower in drug-resistant cells. Gilteritinib did not affect the levels of DOX in the parental cells (Fig. 4C). Verapamil served as the positive control. These experimental data suggest that gilteritinib can increase the concentration of chemotherapeutic drugs in tumor cells that are resistant to multiple drugs. This is accomplished by suppressing the pumping function of the ABCB1 transporter, effectively reversing the effect of MDR on tumors.

### 3.5. Gilteritinib enhances ATP hydrolysis without impacting the expression or subcellular distribution of ABCB1

ATP hydrolysis provides an energy source for ABC transporters to expel substrates. We used ATPase assays to explore the effects of gilteritinib on ATPase activity. We found that gilteritinib increased the ATPase activity of ABCB1 in a concentration-dependent manner. Treatment with gilteritinib using 20 μmol/L increased stimulation by 2.5 times compared to the initial activity (Fig. 5A). These results suggest that gilteritinib can overcome drug resistance by competitively binding to the substrate-binding area of ABCB1. To better understand gilteritinib's mechanism of action, we used western blotting to investigate its impact on ABCB1 protein expression. Fig. 5B shows that the protein expression of ABCB1 remained stable following gilteritinib

administration, independent of the period or concentration of the medication. The effect of gilteritinib on the intracellular distribution of ABCB1 was next examined using immunofluorescence. Fig. 5C shows that ABCB1 (colored red) is evenly distributed across the cell membrane, indicating that gilteritinib (0.3 μM) did not affect its specific location within the cell.

### 3.6. Docking analysis of the binding of gilteritinib with ABCB1 homology model

Tight-binding ligands frequently enhance the thermal stability of target proteins [35]. CETSA, a technique for measuring variations in the temperatures at which proteins melt was used to investigate gilteritinib interacts with the target protein. The results revealed that gilteritinib can make ABCB1 more stable at high temperatures than the solvent control (1 % DMSO) at temperatures of 40, 45, 50, 55, 60, 65, and 70 °C (\*  $p < 0.05$ , \*\*  $p < 0.01$  versus the 40 °C group, Fig. 6A).

To conduct a more detailed analysis of the interactions between gilteritinib and ABCB1, we performed a docking simulation within the ligand-binding region of ABCB1 (residue 7A69). Gilteritinib successfully attached to the ligand binding site, as evidenced by an affinity score of −9.633 kcal/mol. Fig. 6 (B-D) depicts the particular intricacies of the interaction between the ligand and receptor. Gilteritinib interacts with ABCB1 primarily through hydrophobic interactions. Gilteritinib is located within the hydrophobic cavity formed by amino acid residues Phe336, Leu339, Ile340, Phe343, Tyr310, Tyr307, Ile306, Phe303, Tyr953, Tyr950, and Met949. Additionally, Phe728 established pi-cat stacking interactions, which stabilized gilteritinib. Furthermore, the formation of hydrogen bonds between Gln347 and Tyr953 stabilized gilteritinib.

### 3.7. Gilteritinib does not affect AKT or ERK phosphorylation

Downregulation of phosphorylated AKT or ERK levels promotes apoptosis, cell cycle arrest, and senescence in many malignancies. Studies indicate that the activation of AKT and ERK in neoplastic cells can diminish cancer's susceptibility to chemotherapeutic agents [36]. This study further confirms whether Gilteritinib reduces multidrug resistance by activating the AKT and ERK pathways. Western blot tests revealed that the protein levels of AKT, p-AKT, ERK, and p-ERK did not change in cells that were resistant to treatment with different concentrations of gilteritinib (0, 0.3, and 3 μM for 72 h) or for varied lengths of time (0.3 μM for 0, 24, and 72 h) (Fig. 7). This shows that gilteritinib's potential to reverse ABCB1-mediated MDR is unaffected by AKT and ERK signaling pathway suppression.

## 4. Discussion

Chemotherapy is primarily used in the clinical environment to treat malignancies. Nevertheless, MDR enables tumors to develop resistance to a wide spectrum of chemotherapy drugs that act via several pathways, considerably reducing chemotherapy efficacy. Overexpression of ABC transporters is one of the most common mechanisms of MDR. To date, three generations of MDR inhibitors based on ABC transporters have been produced. The insufficient pharmacological conditions, particularly regarding safety, have led to the absence of FDA approval for most of them, thereby restricting their therapeutic application in clinical settings. This underscores the necessity for further investigation into MDR reversal agents with clinical significance [37,38]. Several FLT3 inhibitors (midostaurin, crenolanib, ponatinib, and quizartinib) are substrate and/or inhibitor of ABCB1 and ABCG2 have been reported to interact with ABC transporters in recent years [39–42]. Experiments have shown that these reversal medications can overcome tumor MDR. However, the majority of the ABC transporter inhibitors under investigation are still in preclinical or clinical trials [43]. The FDA and European Medicines Agency (EMA) have approved gilteritinib, an orally

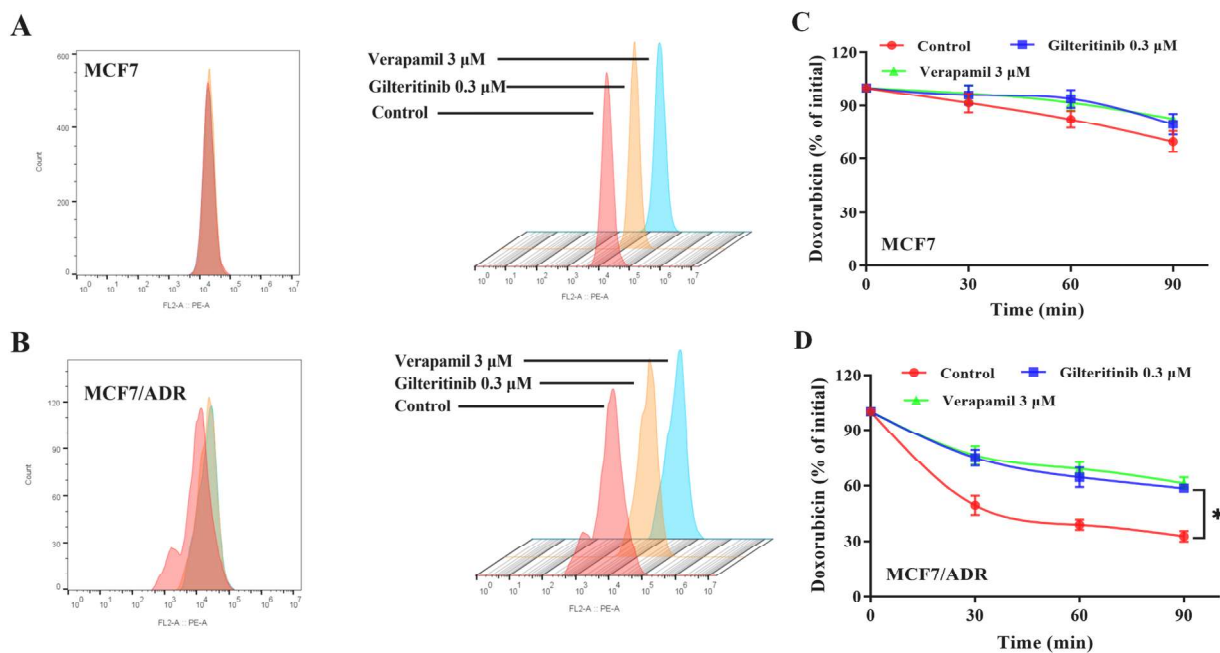


**Fig. 4.** Effects of Gilteritinib on the intracellular accumulation and efflux of substrate drugs in ABCB1-overexpressing MDR cells and parental cells. (A-B) Dox accumulation in MCF7 and MCF7/ADR cells. (C-D) Dox efflux in MCF7 and MCF7/ADR cells. All these experiments were repeated at least three times. Results are mean ± SD. (n = 3). \* p < 0.05 compared with the control group.

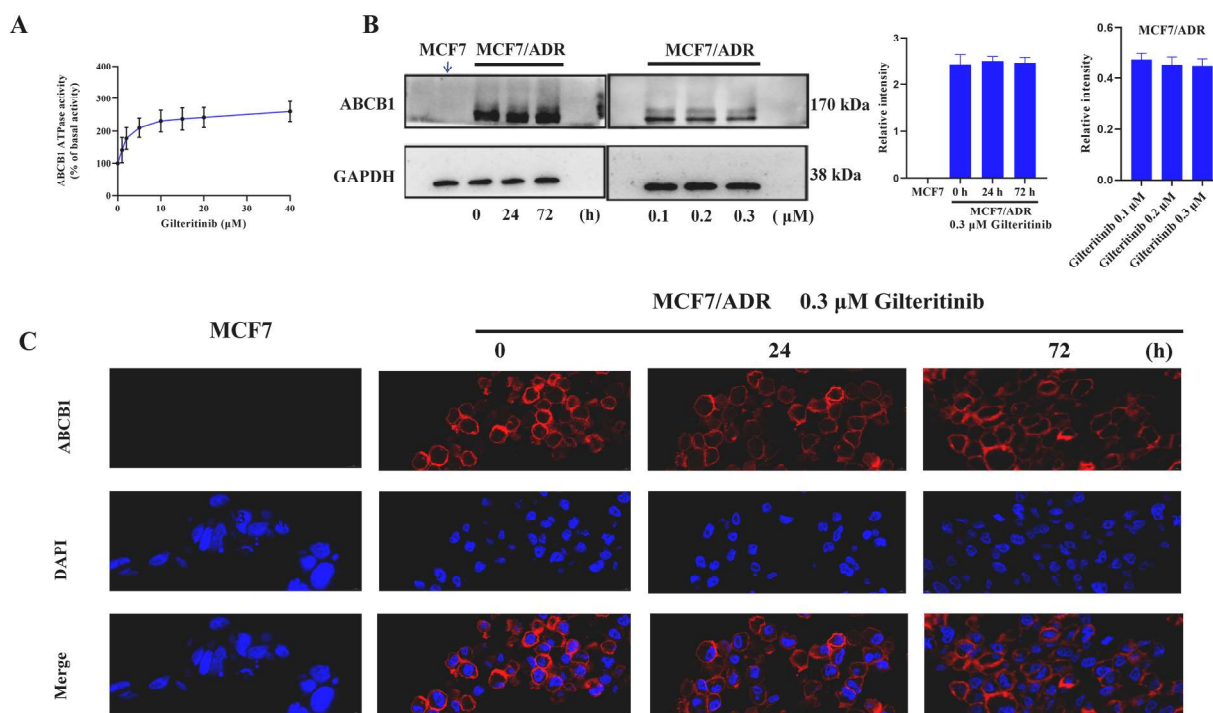


**Fig. 5.** Gilteritinib stimulates the activity of ATPase without altering the expression or subcellular localization of ABCB1. (A) Gilteritinib at concentrations ranging from 0 to 40 μM enhances the activity of ABCB1 ATPase. (B) The impact of incubating MCF7 and MCF7/ADR cells with 0.3 μmol/L Gilteritinib for 0, 24, and 72 hours on the levels of protein expression of ABCB1 or 0.1, 0.2, and 0.3 μmol/L Gilteritinib for 72 hours on the levels of protein expression of ABCB1. (C) The subcellular localization of MCF7 and MCF7/ADR cells after incubation with 0.3 μmol/L Gilteritinib for 0, 24, and 72 hours. The ABCB1 protein is detected by a red signal, while DAPI is detected by a blue signal. The scale bar is 5 μm. All these experiments were repeated at least three times. Data are represented as mean ± SD. (n = 3).

administered small-molecule FLT3 inhibitor, to treat acute myeloid leukemia with FLT3 mutations[27]. Except for research on FLT3-dependent malignancies, there is little evidence on the impact of gilteritinib on MDR cancers. This study sought to determine the efficacy of gilteritinib against ABCB1-mediated MDR *in vitro* and *in vivo* settings.

Initially, we used a CCK8 assay to determine the effect of gilteritinib on cell proliferation. We selected the least harmful gilteritinib concentrations for future studies on drug resistance reversal. This was done to prevent cell growth suppression due to gilteritinib's toxic properties. Drug resistance reversal trials have revealed that gilteritinib can



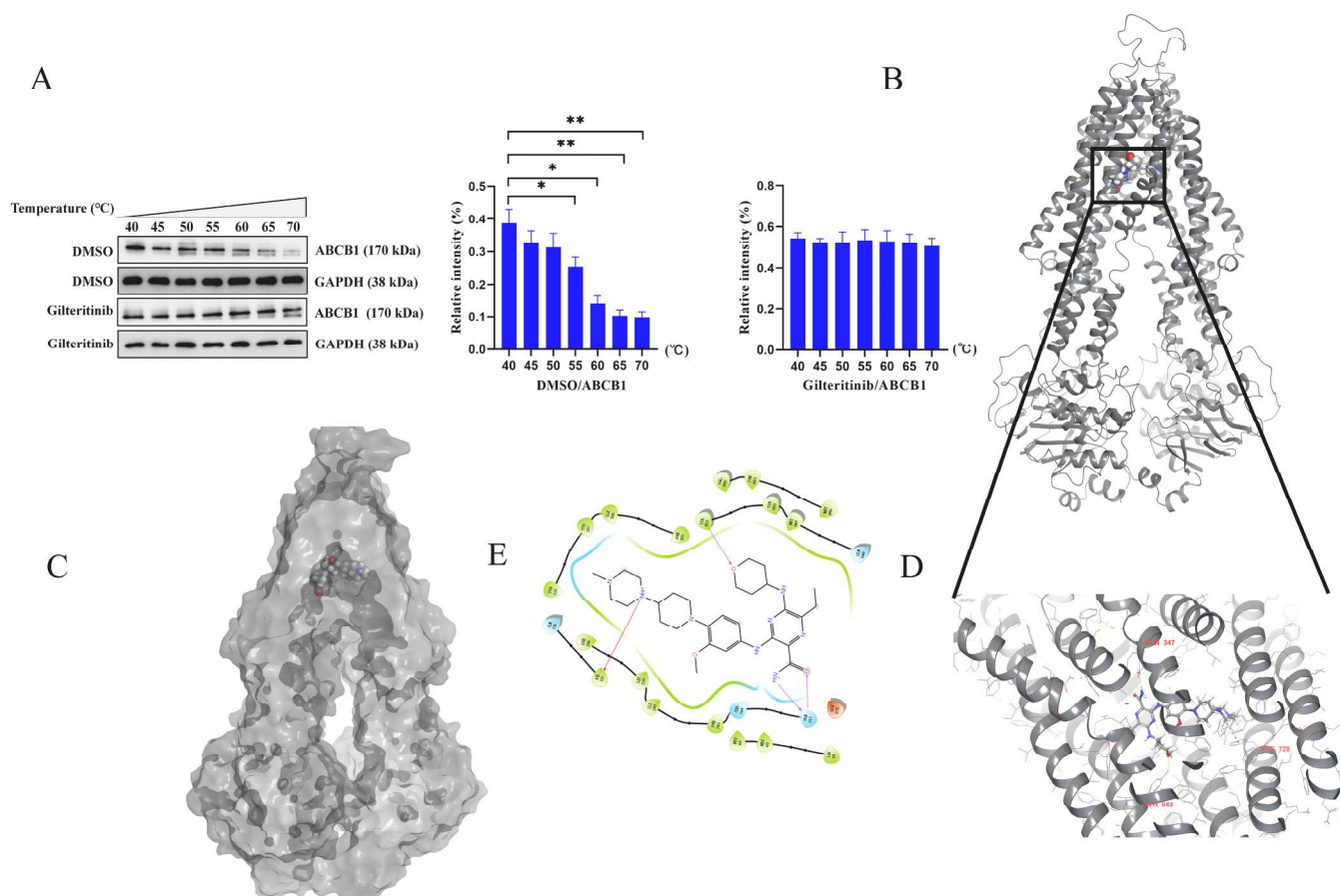


**Fig. 6.** The molecular modeling of Giliteritinib with human ABCB1. (A) The interaction between Giliteritinib and ABCB1 was assessed by a cellular thermal shift assay. The data are presented as mean  $\pm$  SD. (n = 3). \*  $p < 0.05$ , \*\*  $p < 0.01$  versus the 40 °C group. (B) Overview of the best-scoring pose of giliteritinib in the drug binding pocket of ABCB1 protein. ABCB1 was displayed as gray ribbons. Giliteritinib was displayed as colored spheres. (C) Docked complex displayed with protein surface and ligand surface. Giliteritinib was displayed as colored spheres. (D) Details of interactions between giliteritinib and ABCB1 binding pocket. ABCB1 was displayed as gray ribbons. Important residues were displayed as colored sticks (gray: carbon; blue: nitrogen; red: oxygen). Giliteritinib was displayed as colored sticks (gray: carbon; blue: nitrogen; red: oxygen). pi-cat stackings were displayed as green dash lines. Hydrogen bonds were displayed as yellow dash lines. (E) 2D pemigatinib-ABCB1 interaction. Amino acids with 3.0 Å were displayed as color bubbles, cyan indicates polar residues, and green indicates hydrophobic residues. pi-cat stacking interactions are indicated with red lines. Hydrogen bonds are indicated with purple lines.

effectively overcome the resistance of tumors to numerous drugs caused by ABCB1 overexpression. Giliteritinib, in particular, significantly enhanced the inhibitory effect of chemotherapy drugs on the proliferation of MDR cells overexpressing ABCB1 but had little effect on parental cells. Furthermore, these results were confirmed in HEK293/ABCB1 cells that had been genetically modified to express the ABCB1 gene. Cell colony formation studies and 3D sphere experiments revealed that the combined administration of giliteritinib and PTX suppressed the growth of MCF-7/ADR cells. To further evaluate the reversal effect of giliteritinib, we used a transplanted tumor model to investigate its impact on the anti-tumor efficacy of chemotherapeutic drugs in drug-resistant cells. These findings show that the combination of PTX and giliteritinib greatly improves the anti-tumor impact in the MCF7/ADR cell-transplanted tumor model overexpressing ABCB1. Furthermore, the combination medication did not cause any noticeable toxicity in nude mice. These results suggest that giliteritinib can reverse drug resistance in animals with transplanted tumors. This model was effective and safe. In conclusion, giliteritinib greatly increased the antiproliferative effects of chemotherapeutic drugs on drug-resistant cells overexpressing ABCB1, both *in vitro* and *in vivo*.

We evaluated the mechanism of giliteritinib reversal. Our findings show that giliteritinib binds directly to ABCB1 and increases ATP hydrolysis of ABCB1 without changing its protein levels or subcellular localization. Reversing ABCB1-mediated MDR may reduce efflux

activity. Flow cytometry was used to determine the effect of giliteritinib on the accumulation and efflux of substrate chemotherapeutic medicines in cells exhibiting MDR. These findings showed that giliteritinib pretreatment decreased substrate efflux in cells overexpressing ABCB1, increasing accumulation. CETSA and molecular docking experiments were used to ascertain the drug target binding between giliteritinib and ABCB1. According to reports that High-affinity binding enhances thermal stability and promotes interaction with target proteins [44]. CETSA findings showed that giliteritinib effectively improves the thermal stability of ABCB1, implying that it targets ABCB1 in drug-resistant cells. In addition, we performed computational docking research utilizing a human ABCB1 homology model, which allowed us to identify specific residues that Giliteritinib interacts with and gave a high affinity score of  $-9.633$  kcal/mol, suggesting a potential binding affinity between Giliteritinib and the ABCB1 transporter. Furthermore, at concentrations that effectively reversed MDR, giliteritinib had no significant influence on the activation of the AKT and ERK signaling pathways indicates that Giliteritinib's capacity to counteract ABCB1-mediated MDR is unaffected by the suppression of AKT and ERK signaling pathways. In conclusion, giliteritinib offers prospective clinical applications for the treatment of multidrug-resistant tumors, we advocate investigating the integration of giliteritinib into combination therapy, as it may advantage a certain group of patients with malignancies exhibiting over-expression of ABCB1.



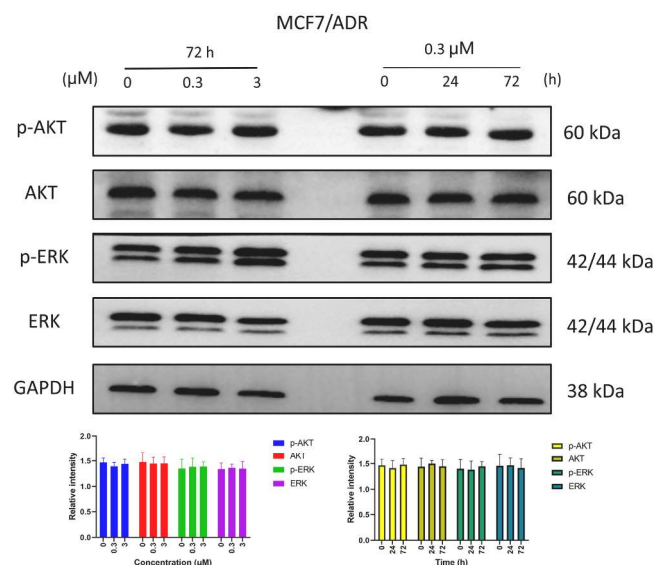


**Fig. 7.** Effects of Gilteritinib on AKT and ERK activation in cancer cells. The impact of Gilteritinib on the expression levels of AKT, ERK, p-AKT, and p-ERK in ABCB1-overexpressing cells at varying concentrations (0, 0.3, and 3  $\mu\text{mol/L}$ ) and for varying durations (0, 24, and 72 h). GAPDH was used as the loading control. All these experiments were repeated at least three times. Data are presented as mean  $\pm$  SD. ( $n = 3$ ).

#### CRedit authorship contribution statement

**Meng Zhang:** Writing – original draft, Project administration, Methodology. **Guang-Hui Ren:** Writing – review & editing, Supervision, Conceptualization. **Shu-Yi Yang:** Writing – review & editing, Supervision, Conceptualization. **Qing-Quan Xiong:** Methodology, Formal analysis. **Xiao-Qi Zeng:** Methodology, Formal analysis. **Jun Chen:** Writing – original draft, Project administration, Methodology. **Mei-Ling She:** Writing – original draft, Project administration, Methodology. **Guo-Bin Qiu:** Writing – review & editing, Supervision, Conceptualization. **Jia-An Ye:** Validation, Software. **Ying-Huan Cen:** Validation, Software.

#### Ethical statement

This article does not include any experiments involving human participants conducted by any of the authors. The Animal Ethics Committee of the Shenzhen Hospital of Southern Medical University approved this animal study (2024-0037).

#### Funding

This research was funded by the National Natural Science Foundation of China (82205108), Guangdong Basic and Applied Basic Research Foundation (2021A1515110963), China Postdoctoral Science Foundation (2022M711539), and Natural Science Foundation of Shenzhen Municipality (JCYJ20220530154005013).

#### Declaration of Competing Interest

The authors declare that they have no known competing financial interests or personal relationships that could have appeared to influence the work reported in this paper.

#### Acknowledgment

The authors thank Dr. Zhe-sheng Chen (St. John's University, NY, USA) for providing HEK293/pcDNA3.1 and HEK293/ABCB1 cell lines.

#### Data availability

Data will be made available on request.

#### References

- [1] X. Zhang, L. Cheng, Y. Lu, J. Tang, Q. Lv, X. Chen, Y. Chen, J. Liu, A MXene-based bionic cascaded-enzyme nanoreactor for tumor phototherapy/enzyme dynamic therapy and hypoxia-activated chemotherapy, *Nanomicro Lett.* 14 (1) (2021) 22.
- [2] Q. Cui, X.L. Liang, J.Q. Wang, J.Y. Zhang, Z.S. Chen, Therapeutic implication of carbon monoxide in drug resistant cancers, *Biochem. Pharmacol.* 201 (2022) 115061.
- [3] Q. Cui, Y. Yang, N. Ji, J.Q. Wang, L. Ren, D.H. Yang, Z.S. Chen, Gaseous signaling molecules and their application in resistant cancer treatment: from invisible to visible, *Future Med. Chem.* 11 (4) (2019) 323–336.
- [4] L. Huang, C. Perrault, J. Coelho-Martins, C. Hu, C. Dulong, M. Varna, J. Liu, J. Jin, C. Soria, L. Cazin, A. Janin, H. Li, R. Varin, H. Lu, Induction of acquired drug resistance in endothelial cells and its involvement in anticancer therapy, *J. Hematol. Oncol.* 6 (2013) 49.
- [5] W. Cui, Q. Dang, C. Chen, W. Yuan, Z. Sun, Roles of circRNAs on tumor autophagy, *Mol. Ther. Nucleic Acids* 23 (2021) 918–929.
- [6] G. Szakács, J.K. Paterson, J.A. Ludwig, C. Booth-Genthe, M.M. Gottesman, Targeting multidrug resistance in cancer, *Nat. Rev. Drug Discov.* 5 (3) (2006) 219–234.
- [7] R.J. Kathawala, P. Gupta, C.R. Ashby Jr., Z.S. Chen, The modulation of ABC transporter-mediated multidrug resistance in cancer: a review of the past decade, *Drug Resist. Updat* 18 (2015) 1–17.
- [8] W. Li, H. Zhang, Y.G. Assaraf, K. Zhao, X. Xu, J. Xie, D.H. Yang, Z.S. Chen, Overcoming ABC transporter-mediated multidrug resistance: molecular mechanisms and novel therapeutic drug strategies, *Drug Resist. Updat* 27 (2016) 14–29.
- [9] L. Gao, Z.X. Wu, Y.G. Assaraf, Z.S. Chen, L. Wang, Overcoming anti-cancer drug resistance via restoration of tumor suppressor gene function, *Drug Resist. Updat* 57 (2021) 100770.
- [10] N. Vasan, J. Baselga, D.M. Hyman, A view on drug resistance in cancer, *Nature* 575 (7782) (2019) 299–309.
- [11] L. Zhang, Y. Li, Q. Wang, Z. Chen, X. Li, Z. Wu, C. Hu, D. Liao, W. Zhang, Z.S. Chen, The P13K subunits, P110 $\alpha$  and P110 $\beta$  are potential targets for overcoming P-gp and BCRP-mediated MDR in cancer, *Mol. Cancer* 19 (1) (2020) 10.
- [12] Y. Zhang, C. Li, C. Xia, K.K. Wah To, Z. Guo, C. Ren, L. Wen, F. Wang, L. Fu, N. Liao, Adagrasib, a KRAS G12C inhibitor, reverses the multidrug resistance mediated by ABCB1 in vitro and in vivo, *Cell Commun. Signal* 20 (1) (2022) 142.
- [13] B. Du, M. Zheng, H. Ma, J. Huang, Q. Jiao, Y. Bai, M. Zhao, J. Zhou, Nanozyme-natural enzymes cascade catalyze cholesterol consumption and reverse cancer multidrug resistance, *J. Nanobiotechnol.* 20 (1) (2022) 209.
- [14] M. Tsukamoto, S. Sato, K. Satake, M. Miyake, H. Nakagawa, Quantitative evaluation of drug resistance profile of cells expressing wild-type or genetic polymorphic variants of the human ABC transporter ABCA4, *Int. J. Mol. Sci.* 18 (7) (2017).
- [15] A. Sajid, S. Lusvarghi, M. Murakami, E.E. Chufan, B. Abel, M.M. Gottesman, S. R. Durell, S.V. Ambudkar, Reversing the direction of drug transport mediated by the human multidrug transporter P-glycoprotein, *Proc. Natl. Acad. Sci. USA* 117 (47) (2020) 29609–29617.
- [16] I. Zimmermann, P. Egloff, C.A. Hutter, F.M. Arnold, P. Stohler, N. Bocquet, M. N. Hug, S. Huber, M. Siegrist, L. Hetemmann, J. Gera, S. Gmür, P. Spies, E. R. Geertsma, R.J. Dawson, M.A. Seeger, Synthetic single domain antibodies for the conformational trapping of membrane proteins, *Elife* 7 (2018).
- [17] P. Gupta, H.L. Gao, Y.V. Ashar, N.M. Karadkhalakar, S. Yoganathan, Z.S. Chen, Ciprofloxacin enhances the chemosensitivity of cancer cells to ABCB1 substrates, *Int. J. Mol. Sci.* 20 (2) (2019).
- [18] F.A. Thélot, W. Zhang, K. Song, C. Xu, J. Huang, M. Liao, Distinct allosteric mechanisms of first-generation Msa inhibitors, *Science* 374 (6567) (2021) 580–585.
- [19] M. Zhang, X.Y. Chen, X.D. Dong, J.Q. Wang, W. Feng, Q.X. Teng, Q. Cui, J. Li, X. Q. Li, Z.S. Chen, NVP-CGM097, an HDM2 inhibitor, antagonizes ATP-binding cassette subfamily B member 1-mediated drug resistance, *Front. Oncol.* 10 (2020) 1219.
- [20] S.M. Stefan, P.J. Jansson, J. Pahnke, V. Namasivayam, A curated binary pattern multitarget dataset of focused ATP-binding cassette transporter inhibitors, *Sci. Data* 9 (1) (2022) 446.
- [21] D. Fan, L. Jiang, Y. Song, S. Bao, Y. Yang, X. Yuan, Y. Zhen, M. Yang, D. Xiong, An Engineered Fusion Protein Anti-CD19(Fab)-LDM Effectively Inhibits ADR-Resistant B Cell Lymphoma, *Front. Oncol.* 9 (2019) 861.
- [22] U. Tidefelt, J. Liliemark, A. Gruber, E. Liliemark, B. Sundman-Engberg, G. Juliusson, L. Stenke, A. Elmhorn-Rosenborg, L. Möllgård, S. Lehman, D. Xu, A. Covelli, B. Gustavsson, C. Paul, P-Glycoprotein inhibitor valspodar (PSC 833) increases the intracellular concentrations of daunorubicin in vivo in patients with P-glycoprotein-positive acute myeloid leukemia, *J. Clin. Oncol.* 18 (9) (2000) 1837–1844.
- [23] S. Mollazadeh, A. Sahebkar, F. Hadizadeh, J. Behravan, S. Arabzadeh, Structural and functional aspects of P-glycoprotein and its inhibitors, *Life Sci.* 214 (2018) 118–123.

- [24] S. Hanigan, J. Das, K. Pogue, G.D. Barnes, M.P. Dorsch, The real world use of combined P-glycoprotein and moderate CYP3A4 inhibitors with rivaroxaban or apixaban increases bleeding, *J. Thromb. Thrombolysis* 49 (4) (2020) 636–643.
- [25] W. Chen, E. Drakos, I. Grammatikakis, E.J. Schlette, J. Li, V. Leventaki, E. Staikou-Drakopoulou, E. Patsouris, P. Panayiotidis, L.J. Medeiros, G.Z. Rassidakis, mTOR signaling is activated by FLT3 kinase and promotes survival of FLT3-mutated acute myeloid leukemia cells, *Mol. Cancer* 9 (2010) 292.
- [26] S.K. Joshi, T. Nechiporuk, D. Bottomly, P.D. Piehowski, J.A. Reisz, J. Pittsenger, A. Kaempf, S.J.C. Gosline, Y.T. Wang, J.R. Hansen, M.A. Gritsenko, C. Hutchinson, K.K. Weitz, J. Moon, F. Cendali, T.L. Fillmore, C.F. Tsai, A.A. Schepmoes, T. Shi, O. A. Arshad, J.E. McDermott, O. Babur, K. Watanabe-Smith, E. Demir, A. D'Alessandro, T. Liu, C.E. Tognon, J.W. Tyner, S.K. McWeeney, K.D. Rodland, B. J. Druker, E. Traer, The AML microenvironment catalyzes a stepwise evolution to gilteritinib resistance, *Cancer Cell* 39 (7) (2021) 999–1014.e8.
- [27] A.E. Perl, G. Martinelli, J.E. Cortes, A. Neubauer, E. Berman, S. Paolini, P. Montesinos, M.R. Baer, R.A. Larson, C. Ustun, F. Fabbiano, H.P. Erba, A. Di Stasi, R. Stuart, R. Olin, M. Kasner, F. Ciceri, W.C. Chou, N. Podoltsev, C. Recher, H. Yokoyama, N. Hosono, S.S. Yoon, J.H. Lee, T. Pardee, A.T. Fathi, C. Liu, N. Hasabou, X. Liu, E. Bahceci, M.J. Levis, Gilteritinib or chemotherapy for relapsed or refractory FLT3-mutated AML, *N. Engl. J. Med.* 381 (18) (2019) 1728–1740.
- [28] A.J. James, C.C. Smith, M. Litzow, A.E. Perl, J.K. Altman, D. Shepard, T. Kadokura, K. Souda, M. Patton, Z. Lu, C. Liu, S. Moy, M.J. Levis, E. Bahceci, Pharmacokinetic Profile of Gilteritinib: a novel FLT-3 tyrosine kinase inhibitor, *Clin. Pharmacokine.* 59 (10) (2020) 1273–1290.
- [29] S. Dhillon, Gilteritinib: first global approval, *Drugs* 79 (3) (2019) 331–339.
- [30] W. Feng, M. Zhang, Z.X. Wu, J.Q. Wang, X.D. Dong, Y. Yang, Q.X. Teng, X.Y. Chen, Q. Cui, D.H. Yang, Erdafitinib antagonizes ABCB1-mediated multidrug resistance in cancer cells, *Front. Oncol.* 10 (2020) 955.
- [31] M. Zhang, X. Zeng, M. She, X. Dong, J. Chen, Q. Xiong, G. Qiu, S. Yang, X. Li, G. Ren, FRAX486, a PAK inhibitor, overcomes ABCB1-mediated multidrug resistance in breast cancer cells, *Braz. J. Med. Biol. Res.* 57 (2024) e13357.
- [32] M. Zhang, M.N. Huang, X.D. Dong, Q.B. Cui, Y. Yan, M.L. She, W.G. Feng, X. S. Zhao, D.T. Wang, Overexpression of ABCB1 confers resistance to FLT3 inhibitor FN-1501 in cancer cells: in vitro and in vivo characterization, *Am. J. Cancer Res.* 13 (12) (2023) 6026–6037.
- [33] Y. Yang, N. Ji, C.Y. Cai, J.Q. Wang, Z.N. Lei, Q.X. Teng, Z.X. Wu, Q. Cui, Y. Pan, Z. S. Chen, Modulating the function of ABCB1: in vitro and in vivo characterization of sitravatinib, a tyrosine kinase inhibitor, *Cancer Commun. (Lond.)* 40 (7) (2020) 285–300.
- [34] M. Mori, N. Kaneko, Y. Ueno, M. Yamada, R. Tanaka, R. Saito, I. Shimada, K. Mori, S. Kuromitsu, Gilteritinib, a FLT3/AXL inhibitor, shows antileukemic activity in mouse models of FLT3 mutated acute myeloid leukemia, *Invest N. Drugs* 35 (5) (2017) 556–565.
- [35] I.F. Sevioukova, T.L. Poulos, Pyridine-substituted desoxyritonavir is a more potent inhibitor of cytochrome P450 3A4 than ritonavir, *J. Med. Chem.* 56 (9) (2013) 3733–3741.
- [36] Q. He, S. Xue, Y. Tan, L. Zhang, Q. Shao, L. Xing, Y. Li, T. Xiang, X. Luo, G. Ren, Dual inhibition of Akt and ERK signaling induces cell senescence in triple-negative breast cancer, *Cancer Lett.* 448 (2019) 94–104.
- [37] W. Ali, G. Spengler, A. Kincses, M. Nové, C. Battistelli, G. Latacz, M. Starek, M. Dąbrowska, E. Honkisz-Orzechowska, A. Romanelli, M.M. Rasile, E. Szymańska, C. Jacob, C. Zwergel, J. Handzlik, Discovery of phenylselenoether-hydantoin hybrids as ABCB1 efflux pump modulating agents with cytotoxic and antiproliferative actions in resistant T-lymphoma, *Eur. J. Med. Chem.* 200 (2020) 112435.
- [38] E. Żesławska, A. Kincses, G. Spengler, W. Nitek, K. Wyrzuc, K. Kieć-Kononowicz, J. Handzlik, The 5-aromatic hydantoin-3-acetate derivatives as inhibitors of the tumour multidrug resistance efflux pump P-glycoprotein (ABCB1): Synthesis, crystallographic and biological studies, *Bioorg. Med. Chem.* 24 (12) (2016) 2815–2822.
- [39] S.H. Hsiao, S. Lusvarghi, Y.H. Huang, S.V. Ambudkar, S.C. Hsu, C.P. Wu, The FLT3 inhibitor midostaurin selectively resensitizes ABCB1-overexpressing multidrug-resistant cancer cells to conventional chemotherapeutic agents, *Cancer Lett.* 445 (2019) 34–44.
- [40] T.J. Mathias, K. Natarajan, S. Shukla, K.A. Doshi, Z.N. Singh, S.V. Ambudkar, M. R. Baer, The FLT3 and PDGFR inhibitor crenolanib is a substrate of the multidrug resistance protein ABCB1 but does not inhibit transport function at pharmacologically relevant concentrations, *Invest N. Drugs* 33 (2) (2015) 300–309.
- [41] R. Sen, K. Natarajan, J. Bhullar, S. Shukla, H.B. Fang, L. Cai, Z.S. Chen, S. V. Ambudkar, M.R. Baer, The novel BCR-ABL and FLT3 inhibitor ponatinib is a potent inhibitor of the MDR-associated ATP-binding cassette transporter ABCG2, *Mol. Cancer Ther.* 11 (9) (2012) 2033–2044.
- [42] J. Bhullar, K. Natarajan, S. Shukla, T.J. Mathias, M. Sadowska, S.V. Ambudkar, M. R. Baer, The FLT3 inhibitor quizartinib inhibits ABCG2 at pharmacologically relevant concentrations, with implications for both chemosensitization and adverse drug interactions, *PLoS One* 8 (8) (2013) e71266.
- [43] E. Weisberg, C. Meng, A.E. Case, M. Sattler, H.L. Tiv, P.C. Gokhale, S.J. Buhrlage, X. Liu, J. Yang, J. Wang, N. Gray, R.M. Stone, S. Adamia, P. Dubreuil, S. Letard, J. D. Griffin, Comparison of effects of midostaurin, crenolanib, quizartinib, gilteritinib, sorafenib and BLU-285 on oncogenic mutants of KIT, CBL and FLT3 in haematological malignancies, *Br. J. Haematol.* 187 (4) (2019) 488–501.
- [44] V.E. Baksheeva, A.V. Baldin, A.O. Zalevsky, A.A. Nazipova, A.S. Kazakov, V. I. Vladimirov, N.V. Gorokhovets, F. Devred, P.P. Philippov, A.V. Bazhin, A. V. Golovin, A.A. Zamyatin Jr., D.V. Zinchenko, P.O. Tsvetkov, S.E. Permyakov, E. Y. Zernii, Disulfide dimerization of neuronal calcium sensor-1: implications for zinc and redox signaling, *Int. J. Mol. Sci.* 22 (22) (2021).